RESEARCH ARTICLE

Time Domain Analysis for Measuring Core Losses in Inductive Elements for Power Electronics: An Investigation Study

MACIEJ CHOJOWSKI[ID]**, MARCIN BASZYŃSKI**[ID]**, (Member, IEEE), ALEKSANDER DZIADECKI, ROMAN DUDEK, AND ANDRZEJ STOBIECKI**[ID]

Department of Power Electronics and Energy Control Systems, AGH University of Science and Technology, 30059 Kraków, Poland

Corresponding author: Maciej Chojowski (chojo@agh.edu.pl)

ABSTRACT The article proposes a method to measure core losses in magnetic elements for medium-frequency power electronics circuits working in conditions close to those in many real industrial circuits: supplied with square-wave voltage and working in linear magnetic region. The article presents analytical considerations regarding the proposed method. The proposed method allows determining core losses in power inductor with only voltage and current measurement - no additional EMF-measuring winding is needed. The method is based on the inductor model, which allows determining losses in the core, while at the same time enables obtaining a time-domain response consistent with rectangular voltage excitation measurements. The method was tested using the real industrial inductor with a copper litz winding and low-loss core (e.g. nanocrystalline core) at various operating points.

INDEX TERMS Inductor losses estimation, inductor losses analysis, core losses.

ABBREVIATIONS

BM	Base method.
CJM	Current jump method.
CSR	Current shunt resistor.
EMF	Electromotive force.
IGSE	Improved Generalized Steinmetz Equation.
WCSE	Waveform-coefficient Steinmetz Equation.

I. INTRODUCTION

The need to precisely determine the value of losses, especially in magnetic elements, is the consequence of the tendency in the construction of power electronic systems to reduce dimensions, weight and cost, and to increase efficiency [1], [2], [3], [4], [5], [6].

The values of magnetic materials parameters given by manufacturers in datasheets usually refer to the conditions of sinusoidal voltage supply [7], [8]. Meanwhile, in modern power electronics systems, the voltage applied to magnetic elements is often in the form of a square wave [7], [9], [10].

To calculate losses in such supply conditions, the modified forms of the Steinmetz equation (improved Generalized Steinmetz Equation (IGSE) [3], [9], [10], [11] or Waveform-coefficient Steinmetz Equation (WCSE) [9]) are used, although satisfactory results are not obtained under all supply conditions [10], [11].

The most reliable results are obtained during measurements under conditions similar to those in which an element will operate [1], [4], [10], [12]. To determine the losses in a magnetic element, one can use well-known methods, which are based on the measurement of electrical quantities (voltage and current) [13], [14] or calorimetric methods [15], [16], [17], [18]. These methods allow the determination of total losses, but usually it is also important to divide them into the so-called core losses and copper losses.

In the case of inductors, the division can be made using the classic two-winding method or special system solutions.

The common practice is the two-winding method, which requires winding an additional winding on the core of the tested power inductor [8], [10], [19], [20], [21], [22], [23], [24]. The additional winding allows the measurement of the induced electromotive force (EMF) and, consequently, the determination of the power dissipated in the core. In addition, the two-winding method is sensitive to phase discrepancy. Phase discrepancy is the difference in phase between the actual inductor current waveform and the measured waveform. This discrepancy usually occurs due to the parasitic inductance of the resistive shunt, the mismatch between the probes and the oscilloscope sampling resolution. The problem becomes especially noticeable at high frequency of waveforms.

Other methods of core losses determination, while eliminating the problem of phase discrepancy, rely on the use of special system solutions [2], [23], [25], [26], [27], [28], [29] which, however, changes the operating conditions of the inductor.

Articles [26], [27] propose methods for canceling the reactive voltage of the tested inductor by connecting a capacitor or another inductor in series. These methods, however, require a very precise selection of the compensation capacitance or inductance value. This is not an easy task. Modifications of reactive voltage compensation methods were proposed in [2] and [28]. In both cases, inductance compensation is implemented, which allows the methods to be used for excitation waveforms of any shape.

According to the method proposed in [25], an air inductor with the same winding is connected in series with the tested core inductor. Simultaneously, separately, calorimetric measurements of losses of both inductors are made and it is assumed that the difference in measured values determines the losses in the core of the tested power inductor

As mentioned earlier, the additional winding for EMF measurement is necessary when measuring core losses with the two-winding method. Currently, with the huge popularity of power electronic systems, their construction usually uses the rich market offer for ready-made inductors, and these often do not allow the winding of the additional measuring winding.

Therefore, it is important to develop a method that allows determining the losses in the core and in the copper of the inductor working in the conditions similar to those in the target system, without the need to modify the inductor or the system in which it operates.

The measurement method presented in this article allows determining the losses in the core and in the copper of the inductor, without the need for changes in the power electronic system or in the inductor itself. The method uses only the measurement of the inductor voltage and the inductor current. It is necessary to use a current and voltage probe with a possibly high bandwidth and high accuracy in order to minimize the implementation error of the developed algorithm.

The method is applicable to cases where the voltage on the tested inductor is rectangular and is forced by an appropriate power electronics system, with the possibility of adjusting both the voltage amplitude and its frequency, while maintaining a constant duty cycle $D = 50\%$. Such excitation corresponds to the operating conditions of the inductor relatively often encountered in practical power electronic systems.

The article has been divided into four parts. Chapter II contains theoretical analysis of the proposed method and basic assumption of power inductor model. Chapter III is devoted to the practical implementation of the method and contains results of core losses measurements. The article ends with a major summary and conclusions in chapter IV.

II. PRINCIPLE OF THE PROPOSED METHOD
A. INDUCTOR MODEL ASSUMPTION
In most power electronic medium frequency converters (10 kHz – 200 kHz), the voltage across the inductor is a square wave, resulting in the flow of current shape close to a triangle (when working in a linear region). The simplest inductor model allowing one to separate the losses in the inductor into winding losses (in copper) and losses in the core, and at the same time allowing a good representation of the current waveform in the time domain, is the model shown in Fig. 1.
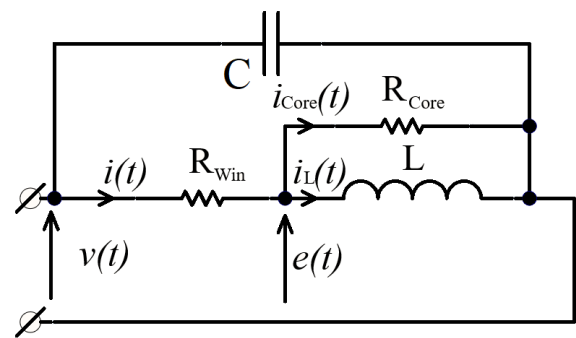

FIGURE 1. Inductor model.

The model contains resistances representing the winding losses (R_{Win}) and the core losses (R_{Core}) with inductor inductance L. In addition, the model has parasitic interturn capacitance (C), which is important in the case of high frequencies and will cause the flow of significant current at a high rate of voltage change (dv/dt) at the inductor terminals. Such a model is not a universal inductor model and in many cases it will be necessary to use a more extended model for precise inductor modeling, e.g. using the Foster or Cauer models [30], [31], [32], [33], [34]. In the next part of the study, the core losses were determined using the model with neglected interturn capacitance C [35] (which is permissible in the frequency range of interest [36], [37]). This model is shown in Fig. 2.

From the differential equations describing this model, in response to a fast change of voltage $v(t)$, one can obtain
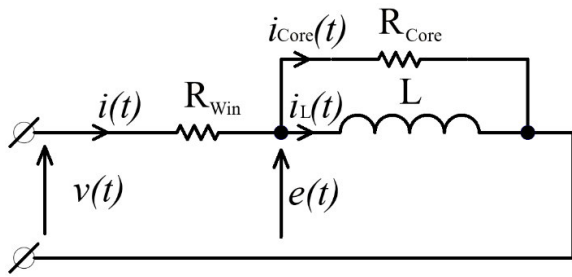
FIGURE 2. Inductor model – equivalent circuit.

expressions on the time waveforms of currents in the following form:

$$i_L(t) = \frac{v}{R_{Win}} + e^{-\frac{t}{\tau}}\left(I_0 - \frac{v}{R_{Win}}\right) \tag{1}$$

$$i_{Core}(t) = -\frac{R_{Win}}{R_{Win}+R_{Core}}e^{-\frac{t}{\tau}}\left(I_0 - \frac{v}{R_{Win}}\right) \tag{2}$$

and the measured inductor current:

$$i(t) = i_{Core}(t) + i_L(t) \tag{3}$$

where: I_o - the initial value of the current in the inductance. The time constant τ is determined by the equation:

$$\tau = L\frac{R_{Win}+R_{Core}}{R_{Win}R_{Core}} = \frac{L}{R_{Win}||R_{Core}} \tag{4}$$

where: $R_{Core}||R_{Win}$ means the parallel connection of R_{Core} and R_{Win}.

If the condition $t \ll \tau$ is satisfied, then the expressions (1) and (2) can be expanded to the Maclaurin series around time $t = 0$. In practical systems this condition is fulfilled. Relations (1) and (2) will simplify current equation to the following form:

$$i_L(t) = \left(1 - \frac{t}{\tau}\right) \cdot i(0) + \frac{V}{R_{Win}}\frac{t}{\tau} \tag{5}$$

$$i_{Core}(t) = -\frac{R_{Win}}{R_{Win}+R_{Core}}(1 - \frac{t}{\tau}) \cdot i(0)$$
$$+ \frac{V}{R_{Win}+R_{Core}}(1 - \frac{t}{\tau}) \tag{6}$$

If the condition $t \ll \tau$ is met, than:

$$1 - \frac{t}{\tau} \approx 1 \tag{7}$$

Thus, equations (5) and (6) can be simplified to the form:

$$i_L(t) = i(0) + \frac{V}{R_{Win}}\frac{t}{\tau} \tag{8}$$

and:

$$i_{Core}(t) = -\frac{R_{Win}}{R_{Win}+R_{Core}} \cdot i(0) + \frac{V}{R_{Win}+R_{Core}} \tag{9}$$

In practically constructed power inductors, there is a design relationship $R_{Core} \gg R_{Win}$. It results from the fact that the inductor's magnetic circuit must be made of a material with

low losses (i.e. large R_{Core} in the equivalent circuit), and the winding must have a relatively low resistance R_{Win} to limit winding losses. Then the expression (9) simplifies to the form:

$$i_{Core}(t) = \frac{V}{R_{Win}+R_{Core}} \tag{10}$$

Further analysis will be carried out with the assumption that the inductor is powered by a square wave voltage with frequency $f_s = 1/T_s$ with $T_s \ll \tau$, which is true in practice, and that the system is in a steady state, that is, for each half-period of the supply voltage, there is the equation:

$$i(t = n \cdot T_s) = i(0) \tag{11}$$

In the following half-periods, the supply voltage is respectively:

$$v(t) = V \text{ for } t = 0 \text{ to } \frac{T_s}{2}$$
$$v(t) = -V \text{ for } t = \frac{T_s}{2} \text{ to } T_s \tag{12}$$

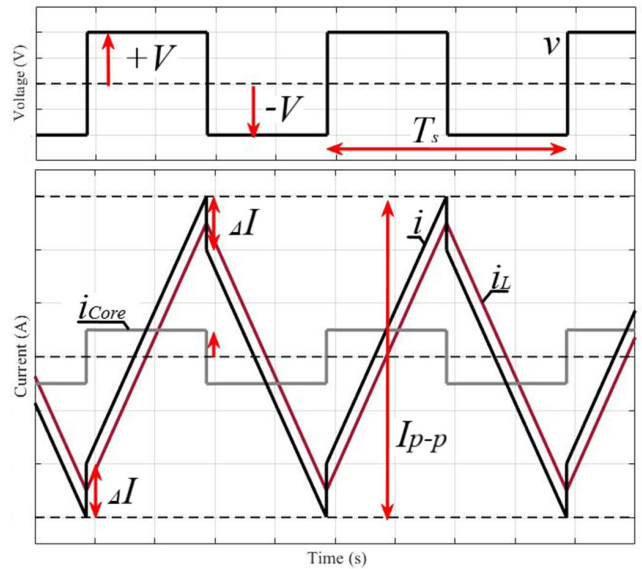Fig. 3 shows the simulation results for a 3-element inductor model (model based on Fig. 2).

FIGURE 3. Inductor voltage and current vs time. The simulation was carried out for the model shown in Fig. 2 with exemplary parameters (shown in Fig. 2): $f_s = 50$ kHz, $L = 100$ uH, $R_{Win} = 0.1$ Ω, $R_{Core} = 100$ Ω and bipolar voltage supply 100 V.

As can be seen, the current step ΔI at the moment of switching the supply voltage is equal to twice the current $i_{Core}(t)$, the value of which can be considered constant during the supply voltage half-period. It results directly from the expression (10). The jump in the current comes only from the change in direction of the current in R_{Core} - a jump in the current time the inductance L is not possible.

B. POWER LOSS CALCULATION

The total power of losses in the reactor is determined by the relationship:

$$\Delta P_c = \frac{1}{T} \int_{t_0}^{T_s+t_0} v(t) \cdot i(t)\, dt \qquad (13)$$

The core losses can be expressed by the following relationships:

$$\Delta P_{core} = \int_{t_0}^{T_s+t_0} i_{Core}(t)^2 R_{Core} dt$$

$$= \frac{1}{T} \int_{t_0}^{T_s+t_0} [e(t) \cdot i_{Core}(t)] dt \qquad (14)$$

To determine this power, it can be assumed with a good approximation that the voltage is equal to EMF $v(t) \approx e(t)$. Consequently according to the current jump method (CJM) the core losses can be calculated:

$$\Delta P_{core-CJM} = \frac{1}{T} \int_{t_0}^{T_s+t_0} v(t) \cdot i_{Core}(t)\, dt$$

$$= V i_{Core}(t) = \frac{1}{2} V \cdot \Delta I \qquad (15)$$

The power balance shows that:

$$\Delta P_{Win} = \Delta P_c - \Delta P_{core} \qquad (16)$$

III. PRACTICAL TESTS OF THE ALGORITHM

A. VARIABLE VOLTAGE AND FREQUENCY CONVERTER

The power supply system for the inductor test is shown in Fig. 4. It consists of a buck converter and a two-level inverter in a bridge system. This power electronic system with suitable control algorithm enables the tested inductor to be supplied with rectangular voltage, with the amplitude regulated by the buck converter and the frequency resulting from the bridge control. The mismatch in the gate – source circuit of the inverter drivers is compensated by additional close-loop, which force DC bias value to 0 A (the duty cycle is 50% +/- 0.5%).

An additional winding was wound on the core of the tested inductor for the sole purpose of verifying the obtained results. The waveforms of the voltage supplying an exemplary inductor, the inductor current and the back electromotive force in the additional winding obtained in this system are shown in Fig. 5.

B. ALGORITHM REALIZATION

The algorithm requires measuring inductor voltage and current waveforms. The algorithm is implemented as follows:

- Zero crossing points and the period T_s (Fig. 5) are determined only from the current waveform.

- The period T_s is divided into two time windows (falling and rising current) and in each of them the approximation of
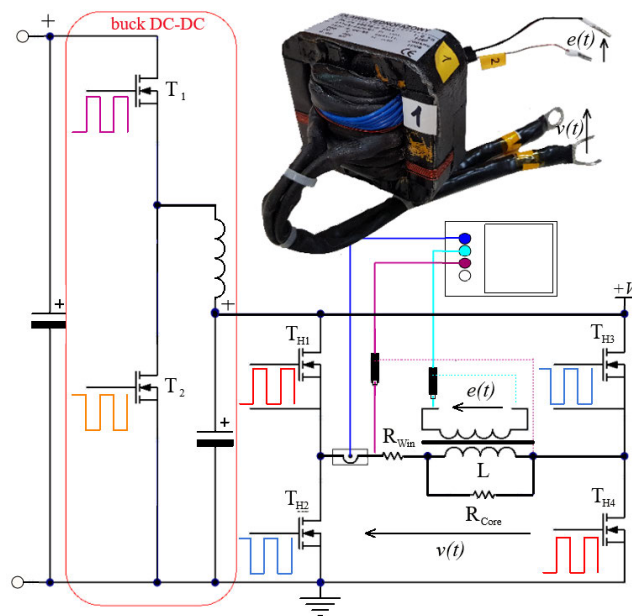

FIGURE 4. Power electronic circuit for generating a rectangular voltage signal for inductors testing - variable DC source and frequency adjuster (Buck converter with H inverter).
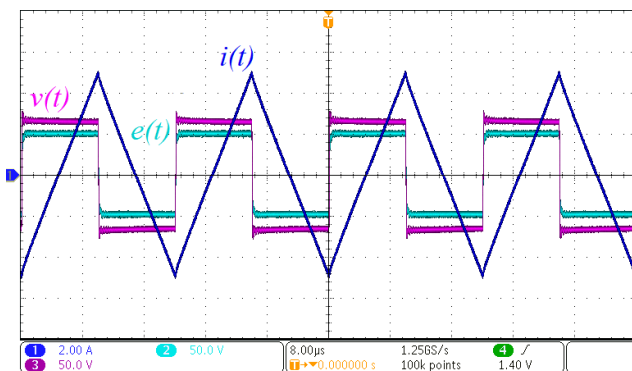

FIGURE 5. Measured inductor current, voltage and EMF. The inductor ($L = 70\ \mu H$) operated with 12 A peak to peak current and at frequency $f_s = 50$ kHz.

the current waveform is performed with the first-degree polynomial. Moreover, the dead time is determined (DT in Fig. 6), and the current waveform in the dead time is approximated by a line parallel to the time axis.

- At the moment of switching, based on the approximation of the current during the dead time and, respectively, the rising or falling current, the current jump ΔI is determined (Fig. 6).

- The inductor current and voltage are measured, and their product for the period T_s (or a finite number of complete periods) is integrated; on this basis the power of total losses ΔP_c is determined from the expression (13),

- ΔP_{core} is determined from the equation (15),

- ΔP_{Win} is determined from the equation (16).

The current waveform at switching (actual measurement data) and the current jump estimation are shown in Fig. 6.

C. THE LIMITATION OF THE PROPOSED METHOD

The proposed method is insensitive to the phase discrepancy error. It is possible because only the voltage *V* value (kept constant during the half period T) and the current jump ΔI during the switching event are measured. The only limitation is to correctly determine the current jump: not only the value of ΔI but also the time point, when the jump occurs. It is significant for the method to measure current with high bandwidth current sensor with low uncertainty.

Except for the errors that can be made with determining the values of voltage, current, and current jump, it is important to remember that not every inductor can be tested, as stated in Chapter II. It is necessary to have the appropriate τ time constant value so that the current waveform is linear with a visible step change.
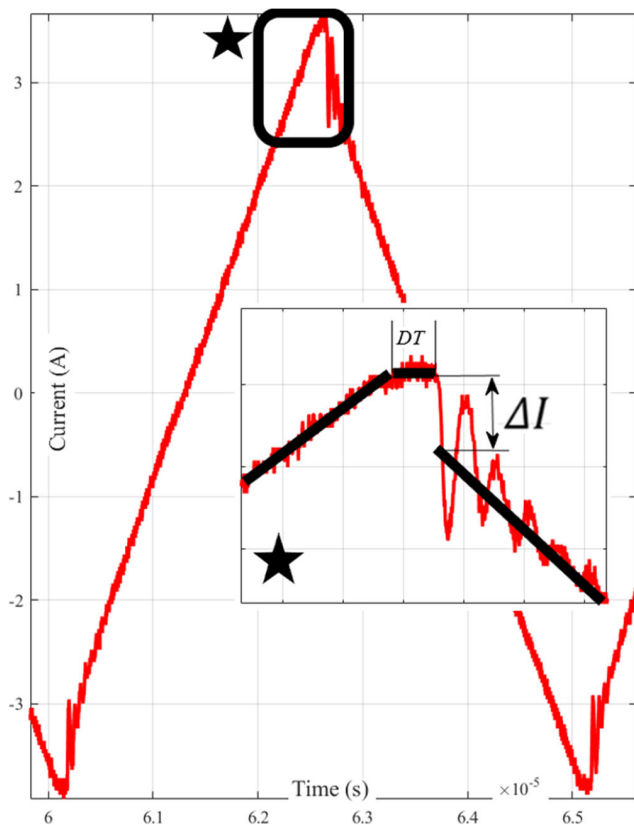

FIGURE 6. Measured current for *L* = 70 μH, peak to peak current I_{pp} equals to 8 A, one period T_s with visible current "jump."

D. EXPERIMENTAL RESULTS

With this method and using the circuit shown in Fig. 4, the power losses were measured for exemplary inductor with a FINEMET core. The selected mechanical and electrical parameters of the inductor are summarized in Table 1.

The measurement system uses a Tektronix measurement set: MDO3104 oscilloscope (with band 1 GHz and 10 million

TABLE 1. Mechanical and electrical parameters of the tested inductor.

Parameter	Value
core type	EC 78/30
weight	~590 g
core dimensions	78 x 74 x 30 mm
gap dimension	2x 0.1 mm + 1x 0.15 mm
wire type	2x (630 x 0.1)
number of turns – main winding (Voltage measurement)	8 turns
number of turns – additional winding (EMF measurement)	8 turns
inductance calculated by supplier	90 μH +/- 10%
maximum DC current	35 A
maximum induction	0.675 T

points record length with 5 GS/s sampling rate), TCP0030A current probe with 120 MHz band and TPP1000 passive probes with the 1 GHz band, which were used to measure the voltage and the back electromotive force. In the measurement system, the voltage is rectangular and as the result the current shape is triangular. As stated in [14], to obtain a loss measurement error of 0.1% with such waveforms, the bandwidth of the measurement system must be at least 5-7 times higher than the switching frequency of the signal. The operating switching frequency of the tested inductors is 50 kHz, so this condition is met.

The inductor has been tested for various values of operating parameters and selected results are presented in Figs. 7 and 8. The figure shows the core losses of the inductive element, determined using two methods:

1. The proposed method, based on the equation (15) - current jump method (CJM),

2. A method based on an additional winding, which allows measurement of EMF – Base Method (BM) [19], [20], [21], [22], [39], [40]:

$$\Delta P_{core-BM} = \frac{1}{T} \int_{t_0}^{T_s+t_0} [e(t) \cdot i(t)]dt \qquad (17)$$

The most frequently emphasized problem in the measurements with the BM, which is also known as the two-winding method is the error in measuring the phase shift between the current and voltage. This so called phase discrepancy, mentioned in the introduction section of this paper, may cause significant error in measurement of the losses [2], [5], [36], [38], [39], [41], [42], [43], [44], [45], [46], [47], [48]. To minimize this error, probes compensation must be applied. In the case of the Tektronix kit mentioned above, compensation is performed after connecting the probes. According to [6], the measurement results using the BM with compensated probes

TABLE 2. General comparison of loss measurement methods for power inductors.

| No.	Method	General remarks	Goal	Signal shape	Measurement device	Additional features of the method	Ref.
1.	Two winding method	Requires winding an additional winding, sensitivity to phase discrepancy	P_{Core} P_{Aux}	triangle with DC bias, D = 50%	oscilloscope, current probe	The use of three DC sources increases the accuracy of measurements	[40]
2.			P_{Core} $P_{Winding}$	triangle with DC bias, D = 50%	oscilloscope, current probe	Triple Pulse Test (TPT) - discontinuous testing procedure. Presented method extends the TPT to include the copper loss so that the total inductor loss is characterized in the procedure	[22]
3.			P_{Core}	square voltage with DC bias	oscilloscope, current probe	An improved core loss separation model enables identifying the hysteresis loss and eddy loss. The loss properties under square waveform are calculated using WCSE equation	[9]
4.	Reactive voltage compensation method	The method is employed to reduce measurement sensitivity to phase errors. It changes the operating conditions of the inductor. Complex designed	P_{total}	various, practical AC waveforms with DC bias	oscilloscope, and CSR	The use of an air core or low loss core transformer to reduce the sensitivity to phase discrepancy. There is a DC current source in the excitation loop. Manual tuning	[46]
5.			P_{Core}	square voltage with DC bias	oscilloscope and CSR	Modified reactive voltage compensation method relies on an implementation of the concept of partial cancellation	[28]
6.			P_{Core}	sinusoidal and rectangular wave excitation	oscilloscope, and CSR	Modified reactive voltage compensation method rely on an implementation of the concept of partial cancellation. No requirement to accurate fine-tune the cancellation component value. The equivalent circuits for both capacitive and inductive cancellation version were considered	[2]
7.	DC measure (differential method)	Measurements or calculations of losses in other elements of the system are the source of error	P_{Core}	symmetrical or asymmetrical square voltage and no DC bias	2 x Fluke 8845A multimeters and ammeter, (no data)	The method consists in measuring the power consumed by the converter loaded with the base air inductor, and then shunting this inductor by the tested inductor and re-measuring. Air inductors, whose loss can be computed precisely, are used to calibrate the inverter's loss. Generally the results of testing are the total inductor losses, but if the inductance of DUT is much larger than the base air inductor, the method measures the inductor core loss directly	[13]
8.			P_{Core}	rectangular voltage, various duty cycle	power meter Yokogawa WT210	Two-step method. Two identical transformers are used, only one is loaded. The core loss and the thermal resistance of the DUT can be computed at one go	[4]
9.	Calorimetric method	Classical calorimetric method is time consuming and essentially aimed at measuring the total inductor loss. It can be used for arbitrary waveform excitation	P_{Core}	any type of excitation, with or without premagnetization	differential scanning calorimeter, IR camera & NTC sensors	Fast transient calorimetric measurement method. Accurate values of the thermal capacitance and the temperature of the core under test are required. The method relies upon the correlation between the measured rate of rise of the core temperature over time, the core thermal capacitance and the introduced losses	[18]
10.			P_{Core}	rectangular voltage with a DC bias	compensation calorimeter	Reducing the measurement time, the measurement period is determined by the time constant of the DUT. Measurements under real application conditions. Measurement of total losses and calculation of winding losses enable evaluation of core losses	[17]
11.			P_{Core} $P_{Winding}$	triangle, with DC bias, D = 2/3	no data	Simultaneous, separate measurements of losses of two inductors connected in series. Changing the operating conditions of the inductor. An air inductor with identical windings is necessary, the same losses in the windings of both inductors are assumed. The method ignores the interaction of the core and the winding	[25]
12.	Mix of methods	Two winding method with specific pulse generation device	P_{Core} $P_{Winding}$	rectangular voltage with DC bias ($D = 50\%$)	oscilloscope, current probe	Two winding method (Triple Pulse Test procedure) for P_{Core}. Special circuit for $P_{Winding}$. The method separates out the winding loss from the core loss through the reactive voltage cancellation concept and this ensures immunity against phase discrepancy error	[5]
13.	Voltage and current measurement		P_{Core}	rectangular or sinusoidal voltage	oscilloscope, current probe & pyrometer	Earlier measurements in the DC circuit allow determining the thermal resistance of the inductor. The method uses thermal properties of the ferrite core. The source of the error is the measurement of the inductor thermal resistances, as well as the simplified method of calculating core loss. Sensitivity to phase discrepancy	[43]
14.		**Proposed method (CJM)**	P_{Core} $P_{Winding}$	**triangle, with DC bias (D = 50%)**	**oscilloscope, current probe**	**Measurement accuracy increases with increasing losses $P_{Winding}$. Required current jump value and current jump point time determination**	-
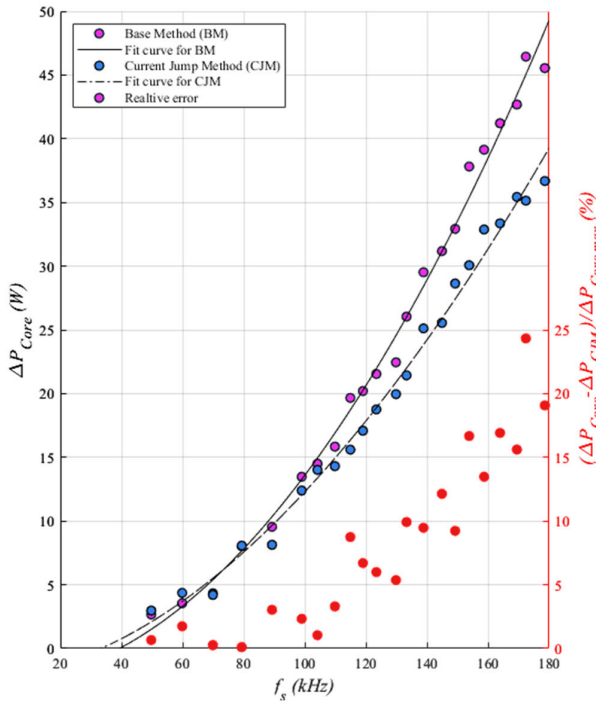
FIGURE 7. Core losses ΔP_{core} vs frequency for tested power inductor. During the tests the peak to peak current was fixed to 8 A.
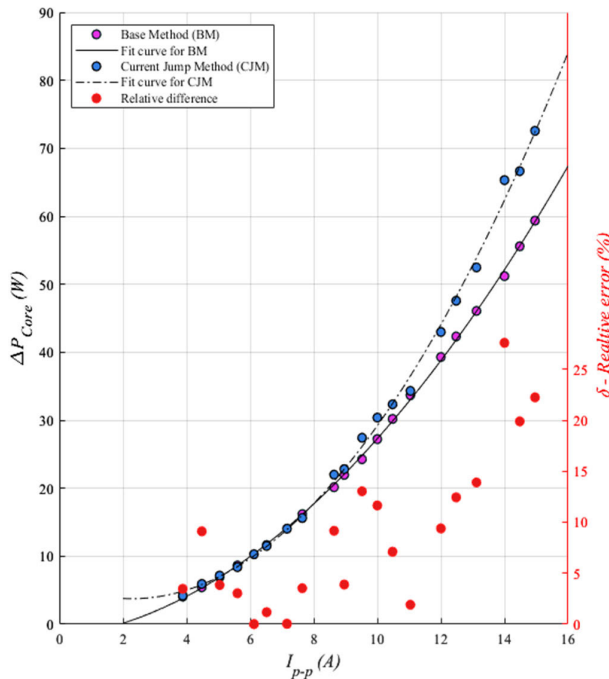

FIGURE 8. Core losses ΔP_{core} vs peak to peak current for tested power inductor. During the tests the frequency was set to 100 kHz.

are very similar to those obtained for the method in which the phase shift measurement error is of minor importance.

Fig. 7 also shows the relative difference in the losses values calculated with both methods for the selected inductor. It was assumed that BM is the reference method.

Additional tests were carried out to verify the algorithm using the same inductor with different peak to peak current and constant frequency (Fig. 8). The results show that in specific range of algorithm application the calculated losses can be close to measured value. In general the method cannot be applied when the core losses are low (no visible current jump). The significant relative error for high loss is caused by low resolution and high range of current and voltage oscilloscope probes. The relative error were calculated by:

$$\delta = \frac{|\Delta P_{core-BM} - \Delta P_{core-CJM}|}{\Delta P_{core-BM}} \cdot 100\% \qquad (18)$$

The defined value of power losses also provides information about inductor parameters (e.g. for model based on Fig. 2). The method allows calculating specific values of both resistances for precision inductor modeling.

IV. CONCLUSION

The presented CJM makes it possible to determine the losses in the inductor core in conditions similar to the operating conditions in real power electronic converters. It is important that the following condition is met: $T_s \ll \tau$ i.e. that the rectangular voltage excitation corresponds to a current close to a triangular one. In the case of relatively small core losses, an increase in the measurement error must be taken into account. It results from the difficulties in determining the moment of switching (current jump event) and the value of the current jump, which are a consequence of the phenomena occurring at the moment of switching (e.g. oscillations shown in Fig. 6).

The Table 2 summarizes all available methods for core losses calculation and measurement. In comparison to other methods, the proposed method in comparison to other methods needs only current (vs time) and voltage (only DC value) measurements (without EMF) to determine the core and winding losses (Table 2).

REFERENCES

[1] A. Bahmani, "Core loss evaluation of high-frequency transformers in high-power DC–DC converters," in *Proc. 13th Int. Conf. Ecol. Vehicles Renew. Energies (EVER)*, Apr. 2018, pp. 1–7.

[2] D. Hou, M. Mu, F. C. Lee, and Q. Li, "New high-frequency core loss measurement method with partial cancellation concept," *IEEE Trans. Power Electron.*, vol. 32, no. 4, pp. 2987–2994, Apr. 2017.

[3] J. Imaoka, W. Yu-Hsin, K. Shigematsu, T. Aoki, M. Noah, and M. Yamamoto, "Effects of high-frequency operation on magnetic components in power converters," in *Proc. IEEE 12th Energy Convers. Congr. Expo.*, Singapore, May 2021, pp. 978–984.

[4] R. Mannam, S. R. Gorantla, and N. Vangala, "A practical technique to measure transformer losses in high frequency SMPS," *Social Netw. Appl. Sci.*, vol. 1, no. 3, pp. 1–12, Mar. 2019.

[5] N. Rasekh, J. Wang, and X. Yuan, "A novel in-situ measurement method of high-frequency winding loss in cored inductors with immunity against phase discrepancy error," *IEEE Open J. Ind. Electron. Soc.*, vol. 2, pp. 545–555, 2021.

[6] D. Rodriguez-Sotelo, M. A. Rodriguez-Licea, I. Araujo-Vargas, J. Prado-Olivarez, A. I. Barranco-Gutiérrez, and F. J. Perez-Pinal, "Power losses models for magnetic cores: A review," *Micromachines*, vol. 13, no. 3, pp. 1–27, Mar. 2022.

[7] H. Matsumori, T. Shimizu, X. Wang, and F. Blaabjerg, "A practical core loss model for filter inductors of power electronic converters," *IEEE J. Emerg. Sel. Topics Power Electron.*, vol. 6, no. 1, pp. 29–39, Mar. 2018.

[8] J. Wang, K. J. Dagan, X. Yuan, W. Wang, and P. H. Mellor, "A practical approach for core loss estimation of a high-current gapped inductor in PWM converters with a user-friendly loss map," *IEEE Trans. Power Electron.*, vol. 34, no. 6, pp. 5697–5710, Jun. 2019.

[9] H. Sun, Y. Li, Z. Lin, C. Zhang, and S. Yue, "Core loss separation model under square voltage considering DC bias excitation," *AIP Adv.*, vol. 10, no. 1, Jan. 2020, Art. no. 015229.

[10] S. Yue, Q. Yang, Y. Li, C. Zhang, and G. Xu, "Core loss calculation of the soft ferrite cores in high frequency transformer under non-sinusoidal excitations," in *Proc. 20th Int. Conf. Electr. Mach. Syst. (ICEMS)*, Sydney, NSW, Australia, Aug. 2017, pp. 1–5.

[11] S. Barg, K. Ammous, H. Mejbri, and A. Ammous, "An improved empirical formulation for magnetic core losses estimation under nonsinusoidal induction," *IEEE Trans. Power Electron.*, vol. 32, no. 3, pp. 2146–2154, Mar. 2017.

[12] L. Yi and J. Moon, "In situ direct magnetic loss measurement with improved accuracy for lossier magnetics," *IEEE Trans. Instrum. Meas.*, vol. 71, pp. 1–14, 2022.

[13] B. Liu, W. Chen, J. Wang, and Q. Chen, "A practical inductor loss testing scheme and device with high frequency pulsewidth modulation excitations," *IEEE Trans. Ind. Electron.*, vol. 68, no. 5, pp. 4457–4467, May 2021.

[14] V. Karthikeyan, S. Rajasekar, S. Pragaspathy, and F. Blaabjerg, "Core loss estimation of magnetic links in DAB converter operated in high-frequency non-sinusoidal flux waveforms," in *Proc. IEEE Int. Conf. Power Electron., Drives Energy Syst. (PEDES)*, Chennai, India, Dec. 2018, pp. 1–5.

[15] F. Grecki and U. Drofenik, "Calorimetric medium frequency loss measurement of the foil inductor winding," in *Proc. IEEE 19th Int. Power Electron. Motion Control Conf. (PEMC)*, Apr. 2021, pp. 611–614.

[16] A. Jafari, M. Heijnemans, R. Soleimanzadeh, R. van Erp, M. S. Nikoo, E. Figini, F. Karakaya, N. Perera, and E. Matioli, "Calibration-free calorimeter for sensitive loss measurements: Case of high-frequency inductors," in *Proc. IEEE 21st Workshop Control Modeling Power Electron. (COMPEL)*, Aalborg, Denmark, Nov. 2020, pp. 1–8.

[17] T. Kleeb, B. Dombert, S. Araújo, and P. Zacharias, "Loss measurement of magnetic components under real application conditions," in *Proc. 15th Eur. Conf. Power Electron. Appl. (EPE)*, Lille, France, Sep. 2013, pp. 1–10.

[18] P. Papamanolis, T. Guillod, F. Krismer, and J. W. Kolar, "Transient calorimetric measurement of ferrite core losses up to 50 MHz," *IEEE Trans. Power Electron.*, vol. 36, no. 3, pp. 2548–2563, Mar. 2021.

[19] A. J. Marin-Hurtado, S. Rave-Restrepo, and A. Escobar-Mejía, "Calculation of core losses in magnetic materials under nonsinusoidal excitation," in *Proc. 13th Int. Conf. Power Electron. (CIEP)*, Guanajuato, Mexico, Jun. 2016, pp. 87–91.

[20] S. Yue, Q. Yang, Y. Li, and C. Zhang, "Core loss calculation for magnetic materials employed in SMPS under rectangular voltage excitations," *AIP Adv.*, vol. 8, no. 5, May 2018, Art. no. 056121.

[21] H. Zhao, H. H. Eldeeb, Y. Zhang, D. Zhang, Y. Zhan, G. Xu, and O. A. Mohammed, "An improved core loss model of ferromagnetic materials considering high-frequency and nonsinusoidal supply," *IEEE Trans. Ind. Appl.*, vol. 57, no. 4, pp. 4336–4346, Jul. 2021.

[22] J. Wang, X. Yuan, and N. Rasekh, "Triple pulse test (TPT) for characterizing power loss in magnetic components in analogous to double pulse test (DPT) for power electronics devices," in *Proc. 46th Annu. Conf. IEEE Ind. Electron. Soc.*, Oct. 2020, pp. 4717–4724, doi: 10.1109/IECON43393.2020.9255039.

[23] A. Huang, X. Wang, H. Zhang, C. Hwang, D. Pommerenke, and J. Fan, "Improved current shunt characterization method for core loss measurement," *IEEE Trans. Power Electron.*, vol. 37, no. 7, pp. 8290–8300, Jul. 2022.

[24] H. P. Rimal, G. Stornelli, A. Faba, and E. Cardelli, "Macromagnetic approach to the modeling in time domain of magnetic losses of ring cores of soft ferrites in power electronics," *IEEE Trans. Power Electron.*, vol. 38, no. 1, pp. 3559–3568, Jan. 2023.

[25] W. Wang, F. Pansier, S. de Haan, and J. A. Ferreira, "Novel and simple calorimetric methods for quantifying losses in magnetic core and GaN transistor in a high frequency boost converter," *Chin. J. Electr. Eng.*, vol. 2, no. 2, pp. 68–75, Dec. 2016.

[26] M. Mu, Q. Li, D. Gilham, F. C. Lee, and K. D. T. Ngo, "New core loss measurement method for high frequency magnetic materials," in *Proc. IEEE Energy Convers. Congr. Expo.*, Sep. 2010, pp. 4384–4389.

[27] M. Mu, F. C. Lee, Q. Li, D. Gilham, and K. D. T. Ngo, "A high frequency core loss measurement method for arbitrary excitations," in *Proc. 26th Annu. IEEE Appl. Power Electron. Conf. Expo. (APEC)*, Mar. 2011, pp. 157–162.

[28] B. N. Sanusi and Z. Ouyang, "Magnetic core losses under square-wave excitation and DC bias in high frequency regime," in *Proc. IEEE Appl. Power Electron. Conf. Expo. (APEC)*, Mar. 2022, pp. 633–639.

[29] Z. Yan, Z. Weibo, and T. Guanghui, "A core loss calculation method for DC/DC power converters based on sinusoidal losses," *IEEE Trans. Power Electron.*, vol. 38, no. 1, pp. 692–702, Jan. 2023.

[30] X. Liu, F. Grassi, G. Spadacini, S. A. Pignari, F. Trotti, N. Mora, and W. Hirschi, "Behavioral modeling of complex magnetic permeability with high-order Debye model and equivalent circuits," *IEEE Trans. Electromagn. Compat.*, vol. 63, no. 3, pp. 730–738, Jun. 2021.

[31] T. Miyazaki, T. Mifune, T. Matsuo, Y. Shindo, Y. Takahashi, and K. Fujiwara, "Equivalent circuit modeling of dynamic hysteretic property of silicon steel under pulse width modulation excitation," *J. Appl. Phys.*, vol. 117, no. 17, May 2015, Art. no. 17D110.

[32] Y. Sato, K. Kawano, D. Hou, J. Morroni, and H. Igarashi, "Cauer-equivalent circuit for inductors considering hysteresis magnetic properties for SPICE simulation," *IEEE Trans. Power Electron.*, vol. 35, no. 9, pp. 9661–9668, Sep. 2020.

[33] Y. Sato, T. Shimotani, and H. Igarashi, "Synthesis of Cauer-equivalent circuit based on model order reduction considering nonlinear magnetic property," *IEEE Trans. Magn.*, vol. 53, no. 6, pp. 1–4, Jun. 2017.

[34] Y. Shindo and O. Noro, "Simple circuit simulation models for eddy current in magnetic sheets and wires," *IEEJ Trans. Fundamentals Mater.*, vol. 134, no. 4, pp. 173–181, 2014.

[35] S. W. Pasko, M. K. Kazimierczuk, and B. Grzesik, "Self-capacitance of coupled toroidal inductors for EMI filters," *IEEE Trans. Electromagn. Compat.*, vol. 57, no. 2, pp. 216–223, Apr. 2015, doi: 10.1109/TEMC.2014.2378535.

[36] F. N. Javidi and M. Nymand, "A new method for measuring winding AC resistance of high-efficiency power inductors," *IEEE Trans. Power Electron.*, vol. 33, no. 12, pp. 10736–10747, Dec. 2018.

[37] M. K. Kazimierczuk, *High-Frequency Magnetic Components*, 2nd ed. Hoboken, NJ, USA: Wiley, 2014.

[38] E. Stenglein, D. Kuebrich, M. Albach, and T. Duerbaum, "Guideline for hysteresis curve measurements with arbitrary excitation: Pitfalls to avoid and practices to follow," in *Proc. Int. Exhib. Conf. Power Electron., Intell. Motion, Renew. Energy Energy Manag.*, Jun. 2018, pp. 1–8.

[39] H. Li, D. Serrano, T. Guillod, E. Dogariu, A. Nadler, S. Wang, M. Luo, V. Bansal, Y. Chen, C. R. Sullivan, and M. Chen, "MagNet: An open-source database for data-driven magnetic core loss modeling," in *Proc. IEEE Appl. Power Electron. Conf. Expo. (APEC)*, Mar. 2022, pp. 588–595, doi: 10.1109/APEC43599.2022.9773372.

[40] M. Baszynski, M. Chojowski, A. Dziadecki, A. Stobiecki, R. Dudek, and J. Skotniczny, "A method and a three source converter for medium frequency magnetic elements losses measurement," *IEEE Trans. Ind. Electron.*, vol. 70, no. 12, pp. 12829–12838, Dec. 2023.

[41] Y. Han and Y.-F. Liu, "A practical transformer core loss measurement scheme for high-frequency power converter," *IEEE Trans. Ind. Electron.*, vol. 55, no. 2, pp. 941–948, Feb. 2008.

[42] D. Sun, W. Fang, J. Lu, X. He, and X. Zhang, "A temperature-controlled system for loss measurement of transformer used in switched-mode power supply," in *Proc. 16th Int. Conf. Electron. Packag. Technol. (ICEPT)*, Changsha, China, Aug. 2015, pp. 118–121.

[43] L. Yi and J. Moon, "Direct in-situ measurement of magnetic loss in power electronic circuits," *IEEE Trans. Power Electron.*, vol. 36, no. 3, pp. 3247–3257, Mar. 2021.

[44] K. Górecki and K. Detka, "Improved method for measuring power losses in the inductor core," *IEEE Trans. Instrum. Meas.*, vol. 70, pp. 1–10, 2021.

[45] C. F. Foo, D. M. Zhang, and X. Li, "A simple approach for determining core-loss of magnetic materials," *J. Magn. Soc. Jpn.*, vol. 22, no. 1, pp. 277–279, 1998.

[46] M. Mu and F. C. Lee, "A new high frequency inductor loss measurement method," in *Proc. IEEE Energy Convers. Congr. Expo.*, Sep. 2011, pp. 1801–1806.

[47] A. Stafiniak and G. Kosobudzki, "Sources of error in AC losses measurement using V–I method," *IEEE Trans. Appl. Supercond.*, vol. 19, no. 3, pp. 3110–3114, Jun. 2009.

[48] Y. Jianying, C. Wei, and H. Jiannong, "A differential method of high-frequency magnetics core loss test scheme," in *Proc. IEEE 5th Int. Symp. Power Electron. Distrib. Gener. Syst. (PEDG)*, Galway, Ireland, Jun. 2014, pp. 1–5.
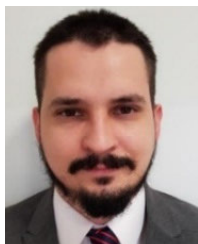
MACIEJ CHOJOWSKI received the Ph.D. degree in electrical engineering from the AGH University of Science and Technology (AGH UST), Kraków, Poland, in 2023. He was a Research and Development Scientist with ABB, for more than one year. Currently, he is an Assistant Professor with AGH UST. His current research interests include the design, construction, and operation of power electronic converters.

MARCIN BASZYŃSKI (Member, IEEE) received the M.S. and Ph.D. degrees in electrical engineering from the AGH University of Science and Technology, Kraków, Poland, in 2001 and 2008, respectively. Since 2006, he has been with the Department of Electrical Drive and Industrial Equipment, AGH University of Science and Technology, as an Assistant Professor. He works on the development of co-simulation tools in the design of the power inverter control systems and solutions initiated to industrial practices in Poland. His current research interests include power electronics and high-speed brushless motor drives.

ALEKSANDER DZIADECKI received the M.S. and Ph.D. degrees in electrical engineering from the AGH University of Science and Technology, Kraków, Poland, in 1974 and 1984, respectively. His current research interests include electric drive and power electronics.

ROMAN DUDEK received the M.S. and Ph.D. degrees in electrical engineering from the AGH University of Science and Technology, Kraków, Poland, in 1980 and 1987, respectively. His current research interests include power electronic traction drives and the control of mining devices.

ANDRZEJ STOBIECKI received the M.S. and Ph.D. degrees in electrical engineering from the AGH University of Science and Technology, Kraków, Poland, in 1982 and 1992, respectively. Since 1982, he has been a Research and Didactic Worker with the AGH University of Science and Technology, conducting classes in the field of electric traction, electric drive, power electronics, mining electrical devices, and electric transport systems.

• • •